Published online 11 November 2009

Nucleic Acids Research, 2010, Vol. 38, No. 2 ***597–607***
doi:10.1093/nar/gkp997

Processing of the *Escherichia coli leuX* tRNA transcript, encoding $tRNA^{Leu5}$, requires either the $3' \rightarrow 5'$ exoribonuclease polynucleotide phosphorylase or RNase P to remove the Rho-independent transcription terminator

Bijoy K. Mohanty and Sidney R. Kushner*

Department of Genetics, University of Georgia, Athens, GA 30605, USA

Received September 21, 2009; Revised October 15, 2009; Accepted October 16, 2009

ABSTRACT

Here we report a unique processing pathway in *Escherichia coli* for $tRNA^{Leu5}$ in which the exoribonuclease polynucleotide phosphorylase (PNPase) removes the Rho-independent transcription terminator from the *leuX* transcript without requiring the RhlB RNA helicase. Our data demonstrate for the first time that PNPase can efficiently degrade an RNA substrate containing secondary structures *in vivo.* Furthermore, RNase P, an endoribonuclease that normally generates the mature 5′-ends of tRNAs, removes the *leuX* terminator inefficiently independent of PNPase activity. RNase P cleaves 4–7 nt downstream of the CCA determinant generating a substrate for RNase II, which removes an additional 3–4 nt. Subsequently, RNase T completes the 3′ maturation process by removing the remaining 1–3 nt downstream of the CCA determinant. RNase E, G and Z are not involved in terminator removal. These results provide further evidence that the *E. coli* tRNA processing machinery is far more diverse than previously envisioned.

INTRODUCTION

The 86 transfer RNA (tRNA) genes in *Escherichia coli* are transcribed either as part of complex operons containing multiple tRNAs, ribosomal RNAs (rRNAs) or messenger RNAs (mRNAs) or as monocistronic transcripts. Irrespective of their physical organization, each precursor tRNA contains extra sequences at both the 5′- and 3′-ends that are removed to generate a mature, functional tRNA. Either RNase E or RNase P are required for the separation of tRNAs that are transcribed as part of polycistronic transcripts to generate pre-tRNAs that become substrates for RNase P, which cleaves them endonucleolytically to generate the mature 5′ termini (1).

While 5′-end processing of all tRNAs has been shown to be catalyzed by only endonucleases, 3′-end maturation is believed to be a multistep process involving both endo- and exoribonucleases (2). For example, for tRNA transcripts terminating with a Rho-independent transcription terminator, an initial endonucleolytic cleavage can remove the stem-loop followed by exonucleolytic trimming to generate the mature 3′ terminus (3–5). In contrast, 3′-end processing can be all exonucleolytic for tRNA transcripts that are terminated in a Rho-dependent fashion (6). Of the eight known $3' \rightarrow 5'$ exoribonucleases in *E. coli*, RNase T and RNase PH are the most important for final 3′-end maturation (7).

Interestingly, polynucleotide phosphorylase (PNPase), a major $3' \rightarrow 5'$ exoribonuclease encoded by *pnp* gene, has only been shown to be involved in shortening of long 3′ trailer sequences (>15 nt) generated after intergenic endonucleolytic cleavages of polycistronic tRNA operons (3,8) or Rho-dependent transcription termination (6). Thus, although PNPase plays a significant role in the processing and degradation of a variety of RNA species (7), its role in tRNA processing and maturation has been thought to be minimal.

Of the eight leucine tRNA genes encoded in *E. coli,* seven are part of five different polycistronic operons that depend on either RNase E or RNase P or both for initial processing and maturation (3–6). Here we describe a unique processing pathway for the eighth leucine tRNA, *leuX* that encodes $tRNA^{Leu5}$. Specifically, PNPase initiates processing by removing the the Rho-independent transcription terminator and stops 1–3 nt downstream of the CCA determinant. This is the first *in vivo* demonstration of processing of an RNA substrate containing a stem-loop structure by PNPase, even though the enzyme has been shown to be inhibited by such structures *in vitro* (9).

*To whom correspondence should be addressed. Tel: +1 706 542 8000; Fax: +1 706 542 3910; Email: skushner@uga.edu

© The Author(s) 2009. Published by Oxford University Press.
This is an Open Access article distributed under the terms of the Creative Commons Attribution Non-Commercial License (http://creativecommons.org/licenses/by-nc/2.5/uk/) which permits unrestricted non-commercial use, distribution, and reproduction in any medium, provided the original work is properly cited.

Endonucleases such as RNase E, RNase G, RNase LS or RNase Z are not involved. Our data further show that RNase P, the endonuclease responsible for generating mature 5′ termini, also removes the terminator from ~10% of primary transcripts by cleaving 4–7 nt downstream of the CCA determinant, generating substrates for RNase II, which removes an additional 3–4 nt. Subsequently, RNase T completes the 3′ maturation process by removing the last 1–3 nt downstream of the CCA determinant left by either PNPase or RNase II.

MATERIALS AND METHODS

Bacterial strains

The *E. coli* strains used in this study were all derived from MG1693 (*thyA715*) (*E. coli* Genetic Stock Center, Yale University). The *rne-1* and *rnpA49* alleles encode temperature sensitive RNase E and RNase P proteins, respectively, that do not support cell viability at 44°C (10–12). SK5665 (*rne-1*) (11), SK2525 (*rnpA49 rbsD296*::Tn*10*) (4), SK2534 (*rne-1 rnpA49 rbsD296*::Tn*10*) (4), SK10019 (*pnpΔ683*) (13), CMA201 (*Δrnb*) (14), SK5726 (*pnp-7 rnb-500*) (15), SK10443 (*rnpA49 rbsD296*::Tn*10 pnpΔ683*) (6), SK7988 (*ΔpcnB*) and SK10148 (*Δrnt*) (4) have been previously described. A P1 lysate grown on SVK53 (MC1061/*ΔrhlB)* was used to transduce both MG1693 and SK10019 (*pnpΔ683*) to construct SK10553 (*ΔrhlB*) and SK10554 (*pnpΔ683 ΔrhlB*), respectively. SVK53 is similar to SVK1 (MC1061/*ΔrhlB)* (16) but has a nearby mini Tn*10* that was used for tetracycline selection. A P1 lysate grown on JW2798 (Keio Collection, Japan) was used to transduce MG1693 and SK2525 (*rnpA49*) to construct SK4390 (*ΔrppH::kan*) and SK4395 (*ΔrppH:kan rnpA49*), respectively. SK2059 (*rnr::kan*) was constructed by P1 mediated transduction using CA265R$^-$ (*rnr::kan*) as the donor strain.

Growth of bacterial strains, isolation of total RNA and northern analysis

Bacterial strains were grown (6) and total RNA was extracted as described previously (17). The RNAs were quantified by measuring the OD_{260} using a Nanodrop (ND1000) apparatus. Total RNA was separated in 6% polyacrylamide gels containing 8 M urea in Tris–Borate–EDTA (TBE) buffer as described previously (6).

Primer extension

Primer extension analysis of the *leuX* transcripts was carried out as described previously (6) with the following modifications. The *leuX* nucleotide sequence was obtained from a PCR DNA product (containing *leuX* genomic sequences) using the Promega *fmol* sequencing kit and the primer LEUX (primer b, Figure 1A) that was also used for the reverse transcription. The sequences were analyzed on a 6% PAGE containing 8M urea.

RT–PCR cloning and sequencing of 5′–3′ ligated transcripts

The 5′- and 3′-ends of *leuX* transcripts were identified by cloning and sequencing the RT–PCR products obtained from 5′→3′ end-ligated circular RNAs following the methods described previously (17). The 5′–3′ junctions of the cDNAs were amplified with a pair of gene-specific primers using GoTaq®Green Master Mix (Promega).

In vitro transcription and RNase E digestion of *leuX* transcripts

The full-length *leuX* runoff transcript was obtained by *in vitro* transcription using a PCR amplified DNA template that contained a modified T7 RNA polymerase promoter. The *leuX* DNA template was amplified using a 5′-primer (T7-LEUX, 5′GGATCCTAATACGACTCACTATA**G**TTTTCCGCATACCTCTTCA3′) and a 3′-primer (LEUX-442, 5′AACACTGGATTTCAGGCATAA3′) that was designed to generate the *leuX* transcript with identical *in vivo* 5′ (+1) end and 3′ Rho-independent transcription terminator. The 5′-primer contained a modified T7 RNA polymerase promoter (underlined) in order to start the transcription at G (bold). The PCR DNA template was purified using PCR purification kit (Qiagen) and used in the *in vitro* transcription reaction with T7 RNA polymerase (Promega) to generate either unlabeled or uniformly labeled (with α-^{32}P-UTP) RNAs. Tri- or monophosphorylated transcripts were generated by adding either GTP or GMP (10-fold in excess), respectively. All transcription reactions generated a single band and were purified using PCR purification column (Qiagen). The unlabeled transcript was used to confirm the 5′ (+1) end by primer extension analysis (data not shown).

His-tagged (carboxy terminus) RNase E was purified from SK10154 (*thyA715 ompT1*::*kan*) and used in the *in vitro* reaction as described previously (18). 9S rRNA precursor substrates were used as control to test the RNase E activity as described before (Chung and Kushner, manuscript in preparation). Two ng of the purified RNase E protein was required to process >50% of 9S rRNA substrate in 4 min at 37°C (data not shown). Either 5′-tri- or 5′ monophosphorylated *leuX* transcripts were assayed in presence of 1–40 ng of RNase E at 37°C. Samples (5 µl) were removed at 0, 2, 4, 8, 16 and 32 min and the reaction was stopped by adding equal volume (5 µl) of 2× RNA loading dye (17). The samples were heated at 65°C for 15 min before separating on a 20% denaturing PAGE/7 M urea. Oligo $(dA)_{10–30}$ (5′-end-labeled with γ-^{32}P-ATP) were used as the molecular weight size standards.

RESULTS

RNase E is not involved in the processing of *leuX* transcript

As part of our efforts to identify every tRNA processing pathway in *E. coli*, we examined the processing of *leuX*, encoding $tRNA^{Leu5}$. This is the only leucine tRNA that is transcribed as a monocistronic transcript and terminates with a putative Rho-independent transcription terminator (Figure 1A) (19). Since previous studies have shown that the Rho-independent transcription terminators associated with many primary tRNA transcripts are removed endonucleolytically by RNase E (3–5) (Table 1),

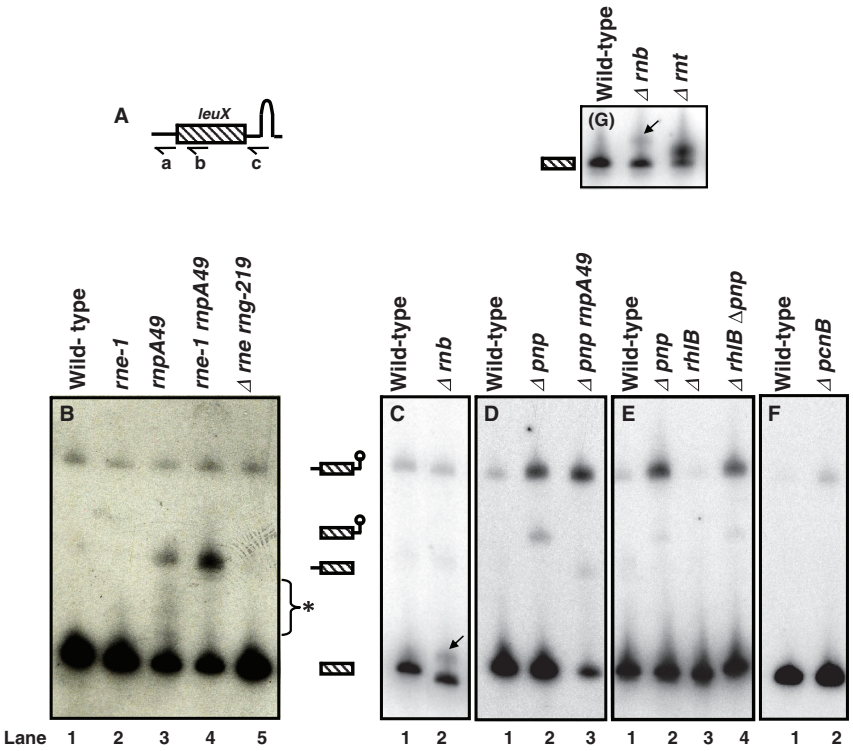

Figure 1. Analysis of the processing of *leuX* transcript. (**A**) Schematic presentation of *leuX* coding sequences (not drawn to scale). Relative positions of the oligonucleotide probes (a, LEUX-UP, 5′ACTGAAGAGGTATGCGGAAA3′; b, LEUX, 5′CGTATTTCTACGGTTGATTTTG3′; and c, LEUX-TER, 5′ACCTCAAGTTGCGGTCTATTTAC3′) used in the northern analysis are shown below the cartoon. (**B–G**) Northern analysis of *leuX* transcript. Total RNA (12 μg/lane) was separated on 6% PAGE, transferred to nylon membrane and probed multiple times with probes a–c as described in the 'Materials and Methods' section. The blots probed with b are shown. The genotypes of the strains used are noted above each lane. The deduced structures of the processing intermediates of *leuX* transcript are shown in between panels B and C. The full-length primary transcripts, which were identical, are not shown in panel G. The apparent difference in the electrophoretic mobility of the mature *leuX* transcript seen in panel C is due to partial bending of the gel during transfer to the membrane.

we hypothesized that RNase E would be required for processing of this transcript.

Accordingly, northern analysis was carried out in strains deficient in RNase E, RNase P or both enzymes, since we anticipated that both enzymes would be required to generate the mature tRNA. Initial probing with a $tRNA^{Leu5}$ specific probe b (Figure 1A) revealed two bands in both the wild-type and *rne-1* strains (Figure 1B, lanes 1–2). The nucleotide composition of both bands was determined by using additional probes that were complementary to the 5′ upstream and 3′ downstream of immature sequences (a,c, Figure 1A). Since probes a and c only hybridized to high molecular weight band (data not shown), this species (~140 nt) was the full-length primary transcript, while the more abundant smaller species represented the 85 nt mature tRNA.

Surprisingly, the relative quantities (RQ) of the primary transcript as well as the mature $tRNA^{Leu5}$ were identical in the wild-type and *rne-1* strains (Figure 1B, lanes 1–2; Table 2). Furthermore, the processed fractions (PFs, defined as the percentage of mature species relative to the total amount of both processed and unprocessed tRNA transcript) were also identical. Since the Rne-1 protein retains significant RNase E activity on tRNA substrates at the nonpermissive temperature (5), we also tested an *rne* deletion strain (*rneΔ1018*) (Chung and Kushner, manuscript in preparation). The complete absence of RNase E also had no effect on the processing of *leuX* transcript (Figure 1B, lane 5; Table 2).

However, in a strain carrying the *rnpA49* allele, thermal inactivation of RNase P led to ~60% reduction in RQ of the mature tRNA, although there was no change the RQ of the primary transcripts (Figure 1B, lane 3, Table 2). In addition, a smear of bands larger than the mature tRNA species appeared under these circumstances (Figure 1B, lane 3, asterisk). The largest of these species was found to contain the 5′ unprocessed end based on its hybridization to probe a and not to probe c (Figure 1A, data not shown). This result was consistent with the RNase P generating the mature 5′ terminus of $tRNA^{Leu5}$. Interestingly, inactivation of both RNase P and RNase E led to disappearance of the majority of the heterogeneous pre-tRNA precursor species (Figure 1B, lane 4, asterisk) except for the species containing the intact 5′-end and a processed 3′-end. In fact, the intensity of this transcript increased ~2.5 ± 0.5-fold compared to the *rnpA49* single mutant (Figure 1B, lanes 3–4) indicating a role for limited RNase E activity within the 5′ leader region resulting in the increased amounts of the heterogeneous tRNA processing intermediates seen in the *rnpA49* single mutant (Figure 1B, compare lanes 3 and 4). Nevertheless, within experimental error, the PF of the

Table 1. Analysis of the Rho-independent transcription terminators associated with tRNA transcripts

Transcripts tRNA	Nucleotide sequence downstream of CCA determinant	Terminator		
		Stem length (nts)	Percentage (GC)	Free energy (kcal)
leuX	CCAAAAGUAUGUAAA	7	57	−9.9
trpT	CCAGAAUCAUCCUUA	9	44	−14
lysQ	CCAAUGUAAAAAAGC	11	45	−14.5
lysV	CCAAUGUAAAAAAGC	11	45	−14.5
proL	CCAAAAAUCCCAAGA	13	31	−15.3
leuZ	CCAUGGGAAAGAUAA	8	50	−15.7
asnV	CCAAAUUCAAAAAAG	12	42	−15.7
proK	CCAAAUUCGAAAAGC	12	42	−16.2
pheU	CCAAAUUCAUAUAAA	11	45	−16.3
glnX	CCACAUUAAAAAAGC	11	45	−16.4
pheV	CCACUAAUUCUUAAG	11	55	−16.5
proM	CCAAUUUUGAACCCC	9	67	−17.0
aspU	CCACUUAUUAAGAAG	14	43	−17.1
alaX	CCAAAUUUCCAACCC	10	70	−18.2
leuU	CCAAAUUCCAGAAAA	13	38	−18.7
serX	CCAUAUUUAAAGAAG	15	33	−19.8
serW	CCAUAUUUAAAGAAG	16	31	−21
aspV	CCACUAUUCACUCAU	12	33	−21.3

The Rho independent transcription terminators associated with the genes shown in bold have been shown to be removed endonucleolytically by RNase E or RNase G.

Table 2. Analysis of *leuX* processing intermediates

Strain genotype	Relative quantity of primary transcript[a]	Relative quantity of mature transcript[a]	PF[b] (%)
Wild-type	1	1	99 ± 1
rne-1	1 ± 0.1	1 ± 0.1	99 ± 1
rnpA49	1 ± 0.1	0.4 ± 0.1	87 ± 3
rne-1 rnpA49	1 ± 0.2	0.4 ± 0.1	85 ± 3
Δrne rng-219	1 ± 0.1	1 ± 0.1	99 ± 1
Δrnb	1 ± 0.1	0.5 ± 0.1	87 ± 3
Δpnp	10 ± 2	1 ± 0.1	80 ± 3
Δpnp rnpA49	10 ± 2	0.1 ± 0.05	40 ± 3
ΔpcnB	2 ± 0.5	0.9 ± 0.1	98 ± 1
ΔrhlB	1 ± 0.1	1 ± 0.1	99 ± 1
Δrnr	1 ± 0.1	1 ± 0.1	99 ± 1
Δrnt	1 ± 0.1	0.3 ± 0.1	30 ± 5

[a]Relative quantities of primary and mature transcripts compared to the wild-type control.
[b]PF is the percentage of mature species relative to the total amount of both processed and unprocessed tRNA transcripts. The data presented represents the average of at least three independent determinations.

mature *leuX* tRNA in both *rnpA49* single and *rnpA49 rne-1* double mutants remained unchanged (Table 2).

The *leuX* Rho-independent transcription terminator is removed independent of RNase G, RNase Z or RNase LS activity

Since we have previously shown some involvement of RNase G in the removal of the terminator from the *secG leuU* transcript (5), we tested a series of isogenic strains carrying various combinations of mutations in RNase G, RNase Z, RNase LS, RNase E and RNase P in case there were redundant processing pathways for *leuX*. Accordingly, we analyzed *rng, rne-1 rng, rnz, rne-1 rnz, rnlA, rne-1 rnlA, rne-1 rng rnz rnlA* and *rne-1 rng rnz rnlA rnpA49* strains. To our surprise, the RQs of the full-length primary transcript and mature tRNA were identical, within experimental error, in all of the strains tested (data not shown).

The *leuX* primary transcript is a substrate for RppH but 5′ dephosphorylation is not required for processing

Recently, it has been shown that the RppH protein converts the 5′ triphosphate terminus of many *E. coli* transcripts to a 5′ phosphomonoester (20), making these RNAs more susceptible to degradation by 5′-end-dependent ribonucleases such as RNase E and RNase G (21–23). Even though neither of these enzymes was involved in *leuX* tRNA processing, we still wanted to investigate if failure to remove the 5′ triphosphate might interfere with *leuX* processing. Total RNA isolated from wild-type, *ΔrppH, rnpA49* and *ΔrppH rnpA49* strains was analyzed by Northern analysis. The RQ and PF of the mature tRNA were comparable in the wild-type and *ΔrppH* strains as well as in the *rnpA49* and *ΔrppH rnpA49 strains* (data not shown).

Even though the absence of RppH did not affect the processing of *leuX,* we tested to see if the *leuX* primary transcript was a substrate for RppH. Since all primary transcripts contain a 5′ triphosphate, the absence of RppH will inhibit self-ligation unless dephosphorylation occurred by an unidentified RNA pyrophosphohydrolase, the transcript was cleaved near the 5′ terminus by an endoribonuclease or was degraded by an *E. coli* functional equivalent of the *B. subtilis* 5′→3′ exonuclease RNase J1 (24). In order to distinguish these possibilities, total RNA isolated from the wild-type and *ΔrppH* strains was self-ligated using T4 RNA ligase. As a control, half of each RNA sample was treated with tobacco acid pyrophosphatase (TAP) to convert the 5′ triphosphate to monophosphate before ligation. The 5′–3′ junctions were reverse transcribed, cloned and sequenced (Figure 2) as

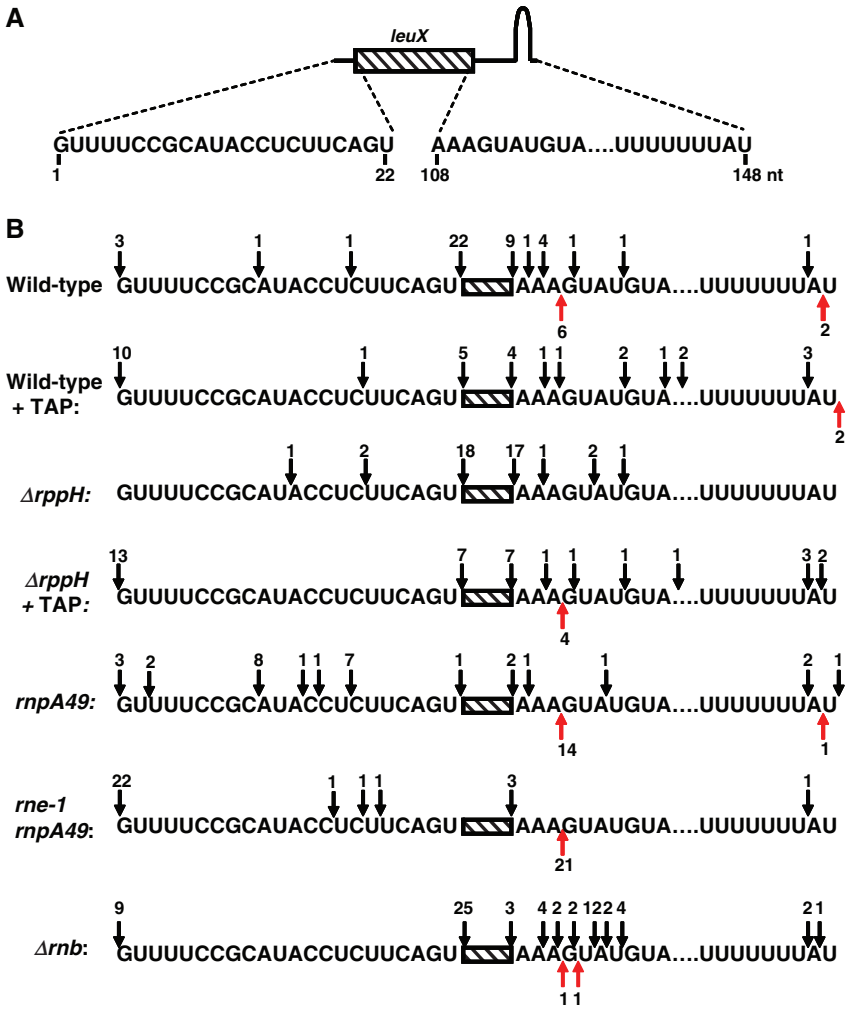

Figure 2. Identification of 5′- and 3′-ends of *leuX* transcripts using RT–PCR cloning of 5′–3′ self-ligated transcripts. The 5′ triphosphate ends of RNAs from selected strains were converted to monophosphate by treating with TAP. (**A**) Schematic presentation of *leuX* coding sequences showing the 5′ upstream and 3′ trailer sequences. A potential Rho-independent transcription terminator at the 3′-end is shown. The nucleotide at the beginning of the transcription start (as identified in Figure 5) is numbered as 1. (**B**) The 5′- and 3′-ends of *leuX* transcripts in wild-type, Δ*rppH*, *rnpA49, rne-1 rnpA49* and Δ*rnb* strains. Each arrow (both black and red) before the nucleotides at 5′-end and after the nucleotides at 3′-end represent a 5′- and 3′-end, respectively. A red arrow indicates the presence of 1–5 non-templated A's after the nucleotide. The numbers directly above or below each arrow represents the number of clones identified with these respective 5′- or 3′-ends.

described in the 'Materials and Methods' section. Without TAP treatment, only ~11% (3/27) of the wild-type clones ligated at the first nucleotide (G) of the primary transcript (19) as compared to 63% (10/16) after TAP treatment. In contrast, none of the clones (0/21) were ligated at the first nucleotide in the *ΔrppH* strain in the absence of TAP treatment. However, ~65% (13/20) of the clones were ligated at the first nucleotide in the *ΔrppH* strain after TAP treatment.

A few of the clones in both genetic backgrounds had 5′-ends upstream of the 5′ mature terminus (Figure 2), which might have arisen from the RNase E cleavages described in Figure 1B. In order to confirm that these species were derived from RNase E cleavages, the 5′–3′ ligated junctions of *leuX* transcripts derived from *rnpA49* single and *rne-1 rnpA49* double mutants were cloned without TAP treatment and sequenced (Figure 2). In the *rnpA49* single mutant ~83% (19/23) of the clones had *leuX* transcripts whose 5′-ends fell between the transcription start site and the mature terminus. In contrast, only ~10% (3/25) of the *leuX* transcripts in *rne-1 rnpA49* double mutant had 5′ truncated ends. In addition, it should be noted that ~88% (22/25) of the *leuX* transcripts isolated from the double mutant ligated at the first nucleotide without TAP treatment indicating the presence of a 5′ monophosphate terminus, which was presumably generated by the action of RppH.

PNPase removes the *leuX* Rho-independent transcription terminator

Since none of the endoribonucleases tested (RNase E, RNase G, RNase LS, RNase Z or RNase P) seemed to have any significant effect on the removal of the *leuX* transcription terminator, we turned our attention to the major

3′→5′ exonucleases present in *E. coli*. While the activities of PNPase, RNase II and RNase T are all strongly inhibited by secondary structures, RNase R has been shown to degrade structured RNA substrates (9,25,26). Northern analysis of *Δrnb, Δrnt*, and *Δrnr* mutant strains showed no effect on the level of the full-length *leuX* transcripts (Figure 1C, Table 2, data not shown). In contrast, the level of the full-length transcript increased 10 ± 2-fold in the *Δpnp* mutant compared to the wild-type control, indicating a significant role of PNPase in the removal of the terminator (Figure 1D, Table 2). In addition, a new minor species that had been processed at the 5′-end but retained the unprocessed 3′ terminator was also identified in the *Δpnp* strain (Figure 1D, lane 2).

The RhlB RNA helicase is not required for PNPase to remove the *leuX* transcription terminator

It has been shown that the RhlB RNA helicase binds directly to PNPase both *in vivo* and *in vitro* and helps promote the degradation of double-stranded RNA degradation by PNPase *in vitro* (27). Accordingly, we anticipated that the RhlB RNA helicase assisted PNPase in the removal of *leuX* transcription terminator. We predicted that the full-length *leuX* primary transcript would accumulate in a *ΔrhlB* strain, comparable to what was observed in the *Δpnp* mutant (Figure 1D, E, lane 2). As shown in Figure 1E (lanes 1–3) and Table 1, the wild-type and *ΔrhlB* strains had almost identical levels of the full-length transcripts. Furthermore, the *leuX* processing pattern in an *ΔrhlB Δpnp* double mutant (Figure 1E, lane 4) was identical to *Δpnp* single mutant (Figure 1E, lane 2).

Polyadenylation by PAP I only has a minor effect on *leuX* tRNA processing

It has been shown that repeated rounds of polyadenylation by PAP I helps PNPase degrade RNA species containing secondary structures *in vitro* (28,29). Since PNPase appeared to be the primary ribonuclease responsible for the removal of the *leuX* Rho-independent transcript terminator, we tested to see if PAP I was required for this reaction. As shown in Figure 1F (lanes 1–2), there was ∼2-fold increase in the level of the full-length transcript in the *ΔpcnB* single mutant compared to the wild-type strain (Table 2). However, the inactivation of both PNPase and PAP I did not increase the level of the full-length transcript compared to the *Δpnp* single mutant (data not shown). While polyadenylation was not required for the efficient removal of the Rho-independent transcription terminator, it was of considerable interest that 33% of the sequenced *leuX* transcripts showed the presence of poly(A) tails (1–5 nt in length) at the 3′ termini of both the processing intermediates and the full-length transcripts in all genetic backgrounds (Figures 2 and 4), but none were found at the mature 3′ terminus.

RNase P also plays a role in the 3′-end processing of *leuX*

Since PNPase was involved in the removal of the 3′ Rho-independent transcription terminator of the *leuX* transcript (Figure 1D, lane 2), we were surprised that the RQ of the mature tRNA was identical in the *Δpnp* and wild-type strains (Table 2). Accordingly, we hypothesized the presence of other ribonuclease(s) that could inefficiently remove the 3′ terminator either in the absence of or in combination with PNPase. As described above, we had not seen any significant effect on terminator removal with RNase II, RNase T, RNase R, RNase E, RNase G, RNase Z, RNase LS or RNase P (Figure 1, data not shown). However, because PNPase was primarily responsible for terminator removal, the role played by a back-up ribonuclease could easily have been overlooked.

Since Nomura and Ishihama (30) suggested, based on *in vitro* experiments, that RNase P might be involved in the processing of both the 5′- and 3′-ends of the *leuX* tRNA, we hypothesized that if RNase P processed both ends of the *leuX* transcript *in vivo,* we should observe a dramatic drop in both the RQ and PF of the mature *leuX* species in an *rnpA49 Δpnp* double mutant compared to either of the single mutants. In fact, both the RQ and PF of the mature tRNA were significantly reduced in the double mutant compared to the single mutants (Figure 1B, lane 3, 1D, lanes 2–3; Table 2). Thus, in the absence of both PNPase and RNase P, the RQ of the mature tRNA was lowered to 10% of the wild-type level whereas only 40% of the tRNA (PF) was matured (Table 2). In contrast, both the *Δpnp* and *rnpA49* single mutants had significantly higher RQ and PF levels of mature tRNA (Table 2).

In order to provide further support for our conclusion that either PNPase or RNase P was required for the removal of the transcription terminator, we measured the half-life of the *leuX* primary transcript. As shown in Figure 3, no full-length transcripts were detected in the wild-type strain indicating its half-life was less than 30 seconds (6). In contrast, the half-life of the primary transcript in the *pnp* deletion strain was 4.9 ± 0.5 min (Figure 3). The half-life was further increased to 6.7 ± 0.5 min in the *Δpnp rnpA49* double mutant (data not shown).

RNase T and RNase II are also required for *leuX* processing

While the RQ of the mature tRNA in the *pnp* deletion strain was identical to the wild-type strain (Figure 1D, lanes 1–2), the PF of the mature tRNA decreased to ∼80%, which was lower than in the *rnpA49* single mutant (Table 2). In contrast, both the RQ and PF of the mature tRNA in the *Δrnt* strains were reduced to 30% of the wild-level (Table 2). These data were consistent with the significant accumulation of 1–3 nt longer precursor products (Figure 1G), presumably dependent on the known role of RNase T in the final 3′-end maturation.

The RQ and PF of the mature tRNA in the *Δrnb* strain were also reduced to 50% and ∼87%, respectively, of the wild-type strain (Table 2), with the concomitant appearance of new processing intermediates which were 3–4 nt longer than the mature tRNA (Figure 1C, lane 2, arrow). These longer processing intermediates were ∼11 ± 2% of the total *leuX* tRNA transcripts in the *Δrnb* strain and were larger than the processing intermediates seen in the *Δrnt* strain (Figure 1G). Furthermore, the levels of the mature tRNA and the 3–4 nt longer unprocessed tRNA

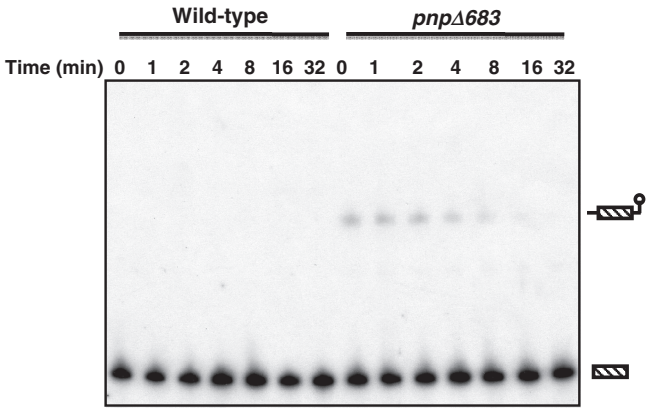

Figure 3. Determination of the half-life for the primary *leuX* transcript. Total RNA (12 μg/lane) from MG1693 (wild-type) and SK10019 (*Δpnp*) was isolated at times (minutes after rifampicin addition) indicated at the top of the blot and was separated on 6% PAGE, transferred to nylon membrane and probed with probe b (Figure 1A) as described in the 'Materials and Methods' section. The intensity of the bands corresponding to the full-length transcript was quantified with a PhosphorImager (Amersham Bioscience) and the values (log of the percentage of transcript remaining) were plotted as a function of time to calculate the half-life.

did not change in a *pnp-7 rnb-500* double mutant compared to the *rnb* deletion strain (data not shown). This suggested no involvement of PNPase in the generation of the longer unprocessed tRNA in the *Δrnb* strain. However, the full-length transcript level in the double mutant increased ~8 ± 2-fold compared to the wild-type and *Δrnb* strains (data not shown), which was consistent with the role played by PNPase in removing the transcription terminator.

In order to characterize the larger processing intermediates, we cloned the 3′–5′ junction of the self-ligated *leuX* tRNA transcripts from the RNase II deletion strain. Eighty-two percent (28/34) of the clones had 3′-ends between the second and seventh nt downstream of CCA, while 75% (21/28) of these ended between fourth and seventh nt (Figure 2). In contrast, majority of *leuX* transcripts with immature 3′ termini in rnb^+ strains contained 1–3 extra nt downstream of CCA (Figure 2). Specifically, in the absence of RNase P (both *rnpA49* and *rnpA49 rne-1*) ~77% (36/49) of the transcripts had immature 3′ termini containing 1–3 nt downstream of the CCA (Figure 2).

The *leuX* transcription terminator has a low predicted free energy

Since PNPase is thought to be strongly inhibited by secondary structures (9), its ability to remove the *leuX* Rho-independent transcription terminator was surprising. In order to confirm that the predicted Rho-independent transcription terminator (Figure 1A) was functional *in vivo*, we cloned and sequenced 5′–3′ junctions of *leuX* transcripts isolated from a *Δpnp* strain. Consistent with the northern analysis, ~57% (13/23) of the clones contained the full-length *leuX* transcript (Figure 4B) compared to only ~11% (3/27) in the wild-type control (Figure 2). Furthermore, ~65% (15/23) of the transcripts terminated in between nucleotides 146–148 which was preceded by a run of 7 Us, consistent with a typical Rho-independent transcription terminator. The rest of the transcripts were processing intermediates, probably derived from the combined action of RNase P and RNase II, with 3′-ends upstream of the terminator.

The predicted secondary structure of the *leuX* 3′ trailer sequence that terminated at nucleotides 146–148 was determined using RNA-STAR program (31). It showed the features of a typical Rho-independent transcription terminator containing a seven nt stem-loop structure with a dyadic stem pairing high in guanine and cytosine residues followed by a uracil-rich stretch (Figure 4C). Since no transcript longer than the 148 nts was detected in any genetic backgrounds (Figures 1, 2 and 4), we conclude that the 3′ secondary structure described in Figure 4C serves as an efficient Rho-independent transcription terminator *in vivo*.

In order to determine why the *leuX* Rho-independent transcription terminator is a substrate for PNPase while other tRNA associated Rho-independent transcription terminators are removed endonucleolytically by either RNase E or RNase G, we compared their relative strength (based on available free energy calculated with RNA-STAR), stem length and percent GC content. Surprisingly, the free energy associated with *leuX* transcription terminator was the lowest of all the terminators tested (Table 1). Furthermore, the lower energy level of the *leuX* terminator seemed to correlate with its shorter stem length rather than its net GC content (Table 1).

RNase E cleaves inefficiently at multiple locations within the 5′ leader region of *leuX* primary transcript when normal processing is impaired by the absence of either RNase P or PNPase

The fact that inactivation of both RNase P and RNase E led to the disappearance of the majority of the smaller pre-tRNA species observed in the *rnpA49* single mutant and 2.5-fold increase in the 5′ unprocessed transcripts (Figure 1B, lanes 3–4, asterisk) suggested that RNase E cleaved inefficiently in the 5′ upstream region of *leuX* precursor tRNA. To provide further support for this hypothesis, primer extension analysis was carried out to identify the precise 5′-ends. Two distinct primer extension products (I and II, Figure 5) were obtained in the wild-type strain. The smaller of the products (II, G) represented the mature 5′-end of *leuX*, while the larger one (I, G) 22 nts upstream of the mature 5′ terminus was identified as the transcription initiation site of *leuX* primary transcript. This result was in agreement with the previous identification of the *leuX* transcription initiation site (19). Consistent with the northern analysis (Figure 1B), the primer extension products in wild-type and *rne-1* strains were at identical locations, but the level of the primer extension product II (mature tRNA) was reduced significantly in the *rnpA49* and *rne-1 rnpA49* mutants (Figure 5). However, the level of the primer extension product I (primary transcripts) increased ~4 ± 1-fold in the *rnpA49* single and ~6 ± 1-fold in the *rne-1 rnpA49* double mutants compared to the wild-type control.

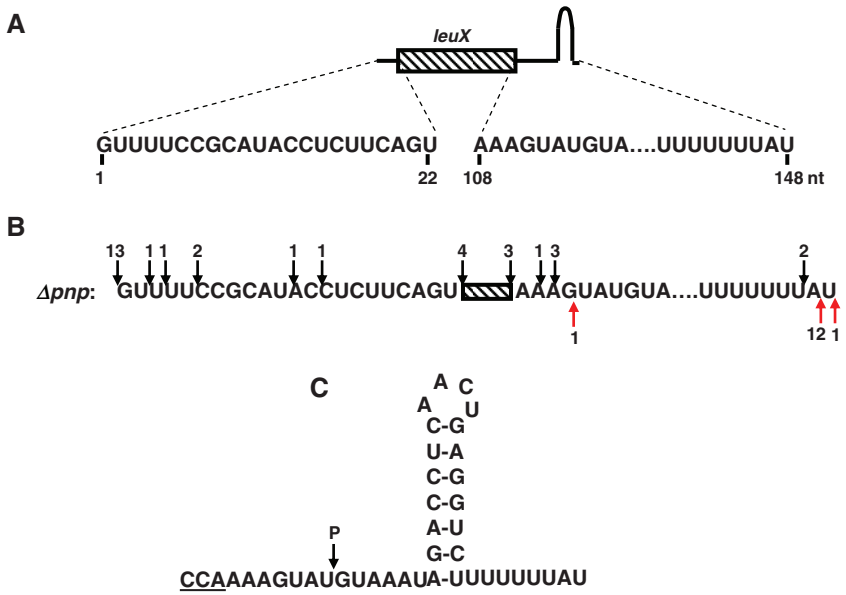

Figure 4. Identification of 5′- and 3′-ends and 3′ Rho-independent transcription terminator of *leuX* transcript in SK10019 (Δ*pnp*) using RT–PCR cloning of 5′–3′ self-ligated transcripts. (**A**) Schematic presentation of *leuX* coding sequences as described in Figure 2A. (**B**) The 5′- and 3′-ends of *leuX* transcripts in Δ*pnp* strain. Arrows are as described in legends to Figure 2B. (**C**) The secondary structure of the Rho-independent transcription terminator as determined by RNA-STAR program (31). The CCA terminus of $tRNA^{Leu5}$ is underlined. P indicates the putative RNase P cleavage site as determined by the *in vitro* studies of Nomura and Ishihama (30).

Furthermore, several additional primer extension products upstream of the mature 5′ terminus (Figure 5, asterisk) were detected in the *rnpA49* single mutant. Most of these termini either disappeared or were significantly reduced in the *rne-1 rnpA49* double mutant.

Analysis of more than 250 5′- to 3′-end-ligated *leuX* transcripts derived from various genetic backgrounds (Figures 2 and 4) showed that many transcripts had truncated 5′-ends that were distributed between 2–16 nt downstream of the transcription start site (Figure 6). Consistent with northern and primer extension analysis (Figures 1 and 5), these 5′ truncated ends were more common in the *rnpA49* and *Δpnp* strains (Figures 2 and 4), but were significantly reduced in an *rne-1* genetic background (Figure 2). Although there were numerous minor cleavages, the major cleavage sites were at 9 and 15 nt downstream of the transcription start site, respectively (Figure 6).

The presence of so many closely spaced cleavage sites in the 5′ upstream region of the transcript (Figure 6) raised the question if RNase E was working exonucleolytically, similar to RNase J1 of *B. subtilis* (24). Even though we did not observe any *in vivo* cleavages after first nucleotide in the cloning and sequencing experiments (compiled in Figure 6), we carried out an *in vitro* kinetic analysis to determine if purified RNase E could degrade a uniformly ^{32}P-labeled *leuX* transcript that had exact 5′ (+1) end of the *in vivo* transcript (see 'Materials and Methods' section). The reaction mixtures were separated on 20% denaturing PAGE/7M urea gels in order to detect the release of any mononucleotides (data not shown). The *leuX* transcript was found to be a very poor substrate for RNase E, since it required 10–20-fold more protein and longer reaction times to observe cleavages compared to a good RNase E substrate (9S rRNA). The major cleavage products were 10, 6 and 4 nt in length and consistent with the *in vivo* findings, a 2 nt fragment was the smallest product that was detected on the gels (data not shown).

DISCUSSION

We describe here a unique PNPase mediated processing pathway for $tRNA^{Leu5}$ (Figure 7) that is distinct from all previously reported RNase E and RNase P dependent tRNA processing pathways (3–6). PNPase degrades the 3′ *leuX* trailer sequences that include the Rho-independent transcription terminator but stops 1–3 nt downstream of the CCA terminus (Figure 7). Alternatively, terminators from ~10% of the primary transcripts are removed by RNase P cleavage at 4–7 nt downstream of the CCA terminus (Figure 7). RNase II cleaves the extra nucleotides at the 3′-end of the RNase P processed transcripts to within 1–3 nt of the CCA terminus. Finally, RNase T removes the last 1–3 nt to generate the mature 3′-end (Figure 7). All the pre-tRNAs, whether they are generated by PNPase or RNase P, have their 5′ termini matured by RNase P. Furthermore, terminator removal precedes 5′ processing.

There are a number of features that make this tRNA processing pathway very unusual. In the first place, since the Rho-independent terminators associated with tRNA transcripts are usually removed endonucleolytically, by either RNase E or RNase G (3–5), it was unexpected that the *leuX* terminator was degraded primarily by a 3′→5′ exonuclease, PNPase. However, the ~10-fold increase in the steady-state level and an almost 10-fold

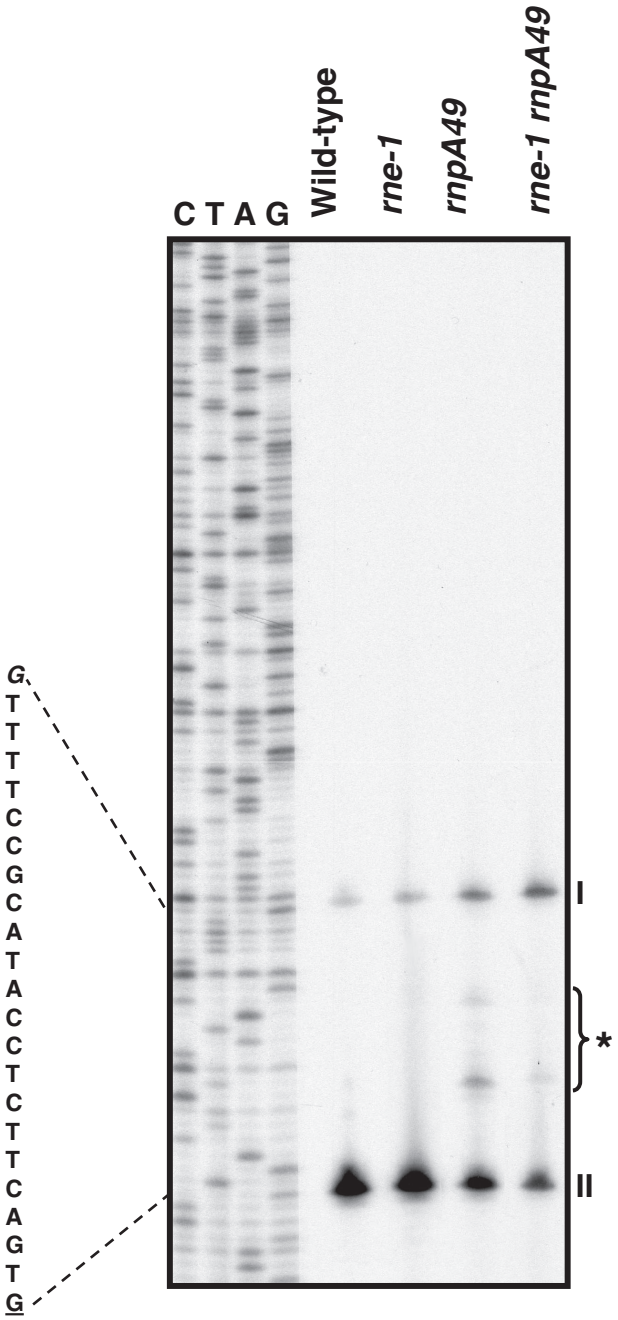

Figure 5. Primer extension analysis of the 5′ upstream region of *leuX* transcript. The reverse transcription products of total RNA (10 μg/lane) isolated from wild-type (MG1693), *rne-1* (SK5665), *rnpA49* (SK2525) and *rne-1 rnpA49* (SK2534) strains using the primer b (Figure 1A) was separated on a 6% PAGE as described in the 'Materials and Methods' section. The CTAG sequencing reactions were carried out using the same primer and a *leuX* PCR DNA fragment as template. The transcription start site (I) and the 5′ mature terminus (II) of *leuX* transcript are indicated. The nucleotide sequences between transcription start (*G*) and the 5′ mature terminus (G) are shown to the left of the autoradiogram. Asterisk indicates the 5′-ends arising from RNase E cleavages.

Figure 6. A schematic presentation of putative RNase E cleavage sites in the 5′ upstream region of *leuX* transcript. The sites were compiled from sequencing data of more than 250 independent clones from various genetic backgrounds. The thickness of each arrow indicates the relative abundance of each cleavage site.

increase in the half-life of the full-length transcript in the *Δpnp* strain clearly demonstrated the requirement of PNPase for terminator removal (Figures 1 and 3; Table 2). Furthermore, the cloning and sequencing of *leuX* species from a *Δpnp* strain confirmed the presence of significantly more transcripts with intact terminators compared to the wild-type control (Figures 2 and 4), while the data derived from the *rnpA49* strains showed that the majority of the PNPase processed species contained an extra 3 nt downstream of the CCA (Figure 2). Furthermore, while the *leuX* terminator (Figure 4C) has a relatively low predicted free energy (Table 1), the sequencing of over 250 *leuX* clones (Figures 2 and 4) demonstrated that this structure functions very efficiently *in vivo*.

Thus, our data represent the first documented example of PNPase degrading through a region of double-stranded RNA *in vivo*. Although PNPase has been shown to be involved in the removal of Rho-dependent transcription terminators (6), its ability to degrade the *leuX* terminator without significant assistance from multiple rounds of polyadenylation of the substrate or through the unwinding activity of the RhlB RNA helicase was surprising because the enzyme is generally inhibited by secondary structures (9,32). However, since the thermodynamic stability of the 7 bp *leuX* stem-loop, which only contains four G/C base pairs (Figure 4C), is relatively low, there may not be a requirement for the unwinding activity of RhlB RNA helicase. In fact, our *in vivo* observations are consistent with previous *in vitro* data showing that stem-loops containing five G/C base pairs are not effective barriers against PNPase degradation (9). Furthermore, Blum *et al.* (29) demonstrated that PNPase could not efficiently degrade the *lpp* Rho-independent transcription terminator (containing a 13 bp stem that includes six G/C base pairs) *in vitro* unless a poly(A) tail longer than five nt was added. Thus, the need for 3′ polyadenylation may be minimized by the presence of 6–8 nt single-stranded region following the *leuX* stem-loop (Figure 4C).

Another interesting feature of this pathway relates to the requirement of RNase II (Figure 1C, lane 2). Many transcripts ended 4–7 nt downstream of the encoded CCA in the RNase II deficient strain (Figure 2) even though PNPase levels are increased 2–3-fold in this genetic background (33). Since PNPase had no difficulty in degrading through the stem-loop structure of the terminator, there was no reason to believe that it stopped at 4–7 nt downstream of the encoded CCA in the absence of RNase II, particularly since most of the immature 3′ termini in the RNase P deficient strains were mapped at 1–3 nt downstream of the CCA terminus (Figure 2). In contrast, a large drop in the RQ and PF of the mature tRNA and the dramatic increase in the half-life of the primary

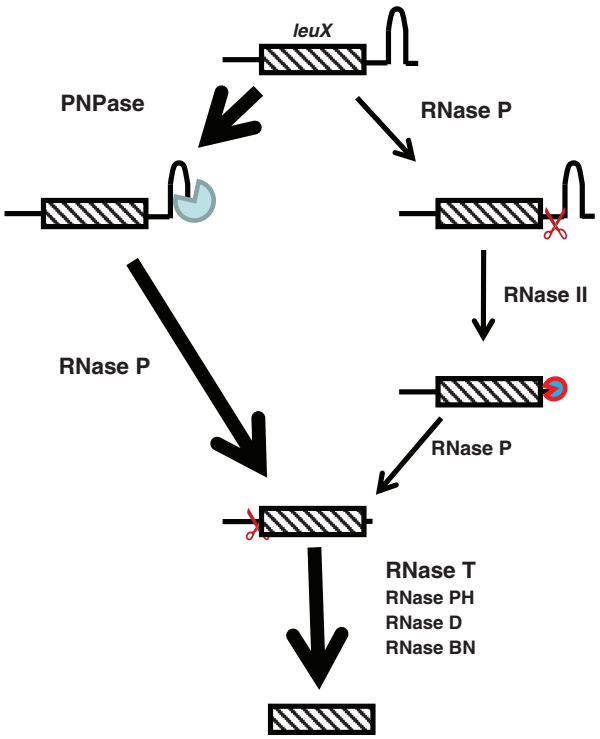

Figure 7. Processing pathways for $tRNA^{Leu5}$ in *E. coli*. PNPase initiates the processing by removing the 3′ trailer sequences that include the Rho-independent transcription terminator up to 1–3 nt downstream of the CCA terminus. Alternatively, RNase P removes the terminator of ~10% of the transcripts by cleaving at 4–7 nt downstream of the CCA terminus. The RNase P cleavage intermediates are substrates for RNase II, which removes 3–4 additional nucleotides. Subsequently, the 5′-end is matured by RNase P and the 3′-end is matured, primarily by the activity of RNase T. However, RNase PH, RNase D, RNase BN and RNase II may substitute in the absence of RNase T (8).

transcript in the *Δpnp rnpA49* strain compared to the *Δpnp* single mutant and wild-type control (Figures 1D,3; data not shown) suggested that the RNase P cleavages at 3′ the ends, left a single-stranded region (~10-11 nt), sufficient for RNase II (34) to bind and remove the next 3–4 nt, but were not substrates for PNPase.

It should also be noted that a previous *in vitro* study mapped a 3′ RNase P cleavage site at 7 nt downstream of CCA (Figure 4C) (30). Thus, it is apparent that the longer processing intermediates in the RNase II deficient strain (Figure 1C) were in fact processed by RNase P, although not as precisely as *in vitro*. While the exact mechanism of how RNase P recognizes cleavage sites in the 3′ trailer sequences is not known, one possible explanation is that a structure different from that shown in Figure 4C forms in a limited number of *leuX* transcripts providing access to RNase P (35). It is not clear if the same RNase P molecule cleaves both the 3′- and 5′-ends of a single transcript. Furthermore, while no other exoribonuclease could replace RNase II in these experiments, it has been shown that all MG1655 derivatives are deficient in RNase PH (36). The final 3′ maturation of $tRNA^{Leu5}$ still requires RNase T, since more than 70% of the precursor tRNA were 1–3 nt longer than the mature tRNA in the *Δrnt* strain (Figure 1G, Table 1).

The detection of some *leuX* primary transcripts in a wild-type strain [Figure 1, (19)] suggests less efficient processing by PNPase compared to terminator removal by either RNase E or RNase G, since primary transcripts processed endonucleolytically are not readily detectable in wild-type strains. In fact, this may be the rate-limiting step during $tRNA^{Leu5}$ processing because 3′-end processing appears to be necessary before RNase P cleavage at the 5′-end (Figure 1). Thus, in the absence of PNPase the major unprocessed species is the full-length *leuX* transcript (Figure 1D, lane 2) with only a minor fraction (<1%) of the processing intermediates having a mature 5′ terminus containing the 3′ terminator sequences. While this result is in contrast to the *in vitro* study of *leuX* processing (19), it is consistent with inhibition of processing of both the *secG leuU* and *metT* operons by RNase P prior to endonucleolytic removal of their respective Rho-independent transcription terminators *in vivo* (5). In contrast, RNase P processing of tRNA transcripts is not inhibited by Rho-dependent transcription terminators (6).

Finally, it should also be noted that previous experiments have shown that RNase E can inefficiently cleave at a limited number of locations within the 5′ upstream region of tRNA transcripts dependent on RNase P for processing (6). Thus, it was not entirely surprising that RNase E inefficiently cleaved the 5′ upstream region of *leuX* transcripts when RNase P was inactivated (Figures 1B and 2). However, what was different in the case of *leuX* was the large number of cleavage sites (Figures 1, 5 and 6) such that it initially appeared as if the enzyme possessed a 5′→3′ exonucleolytic activity similar to what has been observed with RNase J from *B. subtilis* (24). However, a careful combination of the sequencing data (Figures 2 and 4) and *in vitro* analysis of RNase E activity on the full-length *leuX* transcript, demonstrated that this activity is indeed endonucleolytic. In addition, the absence of a role for RppH in $tRNA^{Leu5}$ maturation (data not shown), even though the transcript was a substrate for the enzyme *in vivo*, was consistent with no involvement of the 5′-end-dependent endoribonucleases (RNase E, RNase G) during processing.

Taken together, we have identified a novel tRNA processing pathway that involves primary removal of a Rho-independent transcription terminator by the 3′→5′ exonuclease PNPase. Furthermore, this is the first *in vivo* demonstration that RNase P acts at both the 5′- and 3′-ends of transcripts during tRNA maturation. Surprisingly, when we examined the sequences downstream of the CCA determinant of the Rho-independent transcription terminators presented in Table 1, there was no obvious reason as to why the *leuX* terminator was not a substrate for RNase E. Even though most of the terminators known to be cleaved by RNase E (Table 1, bold type) primarily contain As and Us downstream of the CCA determinant, there are three Gs in the *leuZ* sequence. It thus seems possible that the recognition of individual terminators involves more than primary sequences. If this hypothesis is correct, there could be additional Rho-independent transcription terminator sequences that are not substrates for endonucleolytic cleavage. Taken together, the tRNA

processing pathways in *E. coli* are far more diverse than previously envisioned.

ACKNOWLEDGEMENTS

The authors thank K. Bowden for construction of the *ΔrppH* strains. SVK53 and CA265R$^-$ were kindly provided by A.J. Carpousis and M. Deutscher, respectively.

FUNDING

National Institutes of General Medical Sciences (GM75220 and GM81554 to S.R.K.). Funding for open access charge: National Institutes of Health grant.

Conflict of interest statement. None declared.

REFERENCES

1. Altman,S., Kirsebom,L. and Talbot,S. (1995) Recent studies of RNase P. In Soll,D. and RajBhandary. (eds), *tRNA: Structure and Function*. American Society for Microbiology Press, Washington, DC, pp. 67–78.
2. Morl,M. and Marchfelder,A. (2001) The final cut. The importance of tRNA 3′-processing. *EMBO Rep.*, **2**, 17–20.
3. Li,Z. and Deutscher,M.P. (2002) RNase E plays an essential role in the maturation of *Escherichia coli* tRNA precursors. *RNA*, **8**, 97–109.
4. Ow,M.C. and Kushner,S.R. (2002) Initiation of tRNA maturation by RNase E is essential for cell viability in *Escherichia coli*. *Genes Dev.*, **16**, 1102–1115.
5. Mohanty,B.K. and Kushner,S.R. (2008) Rho-independent transcription terminators inhibit RNase P processing of the *secG leuU* and *metT* tRNA polycistronic transcripts in *Escherichia coli*. *Nucleic Acids Res.*, **36**, 364–375.
6. Mohanty,B.K. and Kushner,S.R. (2007) Ribonuclease P processes polycistronic tRNA transcripts in *Escherichia coli* independent of ribonuclease E. *Nucleic Acids Res.*, **35**, 7614–7625.
7. Deutscher,M.P. (2006) Degradation of RNA in bacteria: comparison of mRNA and stable RNA. *Nucleic Acids Res.*, **34**, 659–666.
8. Li,Z. and Deutscher,M.P. (1996) Maturation pathways for *E. coli* tRNA precursors: a random multienzyme process *in vivo*. *Cell*, **86**, 503–512.
9. Spickler,C. and Mackie,G.A. (2000) Action of RNase II and polynucleotide phosphorylase against RNAs containing stem-loops of defined structure. *J. Bacteriol.*, **182**, 2422–2427.
10. Schedl,P. and Primakoff,P. (1973) Mutants of *Escherichia coli* thermosensitive for the synthesis of transfer RNA. *Proc. Natl Acad. Sci. USA*, **70**, 2091–2095.
11. Arraiano,C.M., Yancey,S.D. and Kushner,S.R. (1988) Stabilization of discrete mRNA breakdown products in *ams pnp rnb* multiple mutants of *Escherichia coli* K-12. *J. Bacteriol.*, **170**, 4625–4633.
12. Ono,M. and Kuwano,M. (1979) A conditional lethal mutation in an *Escherichia coli* strain with a longer chemical lifetime of mRNA. *J. Mol. Biol.*, **129**, 343–357.
13. Mohanty,B.K. and Kushner,S.R. (2003) Genomic analysis in *Escherichia coli* demonstrates differential roles for polynucleotide phosphorylase and RNase II in mRNA abundance and decay. *Mol. Microbiol.*, **50**, 645–658.
14. Piedade,J., Zilhao,R. and Arraiano,C.M. (1995) Construction and characterization of an absolute deletion of *Escherichia coli* ribonuclease II. *FEMS Microbiol. Lett.*, **127**, 187–193.
15. Donovan,W.P. and Kushner,S.R. (1986) Polynucleotide phosphorylase and ribonuclease II are required for cell viability and mRNA turnover in *Escherichia coli* K-12. *Proc. Natl Acad. Sci. USA*, **83**, 120–124.
16. Khemici,V., Toesca,I., Poljak,L., Vanzo,N.F. and Carpousis,A.J. (2004) The RNase E of *Escherichia coli* has at least two binding sites for DEAD-box RNA helicases: functional replacement of RhlB by RhlE. *Mol. Microbiol.*, **54**, 1422–1430.
17. Mohanty,B.K., Giladi,H., Maples,V.F. and Kushner,S.R. (2008) Analysis of RNA decay, processing. amd polyadenylation in *Eschericha coli* and other prokaryotes. In Arraiano,C.M. and Maquat,L. (eds), *Methods Enzymol*, Vol. 447. Academic Press, pp. 3–29.
18. Perwez,T. and Kushner,S.R. (2006) RNase Z in *Escherichia coli* plays a significant role in mRNA decay. *Mol. Microbiol.*, **60**, 723–737.
19. Nomura,T., Fujita,N. and Ishihama,A. (1987) Expression of the *leuX* gene in *Escherichia coli*: Regulation at transcription and tRNA processing steps. *J. Mol. Biol.*, **197**, 659–670.
20. Deana,A., Celesnik,H. and Belasco,J.G. (2008) The bacterial enzyme RppH triggers messenger RNA degradation by 5′ pyrophosphate removal. *Nature*, **451**, 355–358.
21. Tock,M.R., Walsh,A.P., Carroll,G. and McDowall,K.J. (2000) The CafA protein required for the 5′-maturation of 16S rRNA is a 5′-end-dependent ribonuclease that has context-dependent broad sequence specificity. *J. Biol. Chem.*, **275**, 8726–8732.
22. Mackie,G.A. (1998) Ribonuclease E is a 5′-end-dependent endonuclease. *Nature*, **395**, 720–723.
23. Mackie,G.A. (2000) Stabilization of circular *rpsT* mRNA demonstrates the 5′-end dependence of RNase E action *in vivo*. *J. Biol. Chem.*, **275**, 25069–25072.
24. Mathy,N., Benard,L., Pellegrini,O., Daou,R., Wen,T. and Condon,C. (2007) 5′-to-3′ exoribonuclease activity in bacteria: role of RNase J1 in rRNA maturation and 5′ stability of mRNA. *Cell*, **129**, 681–692.
25. Vincent,H.A. and Deutscher,M.P. (2006) Substrate recognition and catalysis by the exoribonuclease RNase R. *J. Biol. Chem.*, **281**, 29769–29775.
26. Zuo,Y. and Deutscher,M.P. (2002) The physiological role of RNase T can be explained by its unusual substrate specificity. *J. Biol. Chem.*, **277**, 29654–29661.
27. Liou,G-G., Chang,H.-Y., Lin,C.S. and Lin-Chao,S. (2002) DEAD box RhlB RNA helicase physically associates with exoribonuclease PNPase to degrade double-stranded RNA independent of the degradosome-assembling region of RNase E. *J. Biol. Chem.*, **277**, 41157–41162.
28. Coburn,G.A., Miao,X., Briant,D.J. and Mackie,G.A. (1999) Reconstitution of a minimal RNA degradosome demonstrates functional coordination between a 3′ exonuclease and a DEAD-box RNA helicase. *Genes Dev.*, **13**, 2594–2603.
29. Blum,E., Carpousis,A.J. and Higgins,C.F. (1999) Polyadenylation promotes degradation of 3′-structured RNA by the *Escherichia coli* mRNA degradosome *in vitro*. *J. Biol. Chem.*, **274**, 4009–4016.
30. Nomura,T. and Ishihama,A. (1988) A novel function of RNase P from *Escherichia coli*: processing of a suppressor tRNA precursor. *EMBO J.*, **7**, 3539–3545.
31. Gultyaev,A.P., van Batenburg,F.H.D. and Pleij,C.W.A. (1995) The computer simulation of RNA folding pathways using a genetic algorithm. *J. Mol. Biol.*, **250**, 37–51.
32. Coburn,G.A. and Mackie,G.A. (1998) Reconstitution of the degradation of the mRNA for ribosomal protein S20 with purified enzymes. *J. Mol. Biol.*, **279**, 1061–1074.
33. Zilhao,R., Cairrao,R., Régnier,P. and Arraiano,C.M. (1996) PNPase modulates RNase II expression in *Escherichia coli*: Implications for mRNA decay and cell metabolism. *Mol. Microbiol.*, **20**, 1033–1042.
34. Frazao,C., McVey,C.E., Amblar,M., Barbas,A., Vonrhein,C., Arraiano,C.M. and Carrondo,M.A. (2006) Unravelling the dynamics of RNA degradation by ribonuclease II and its RNA-bound complex. *Nature*, **443**, 110–114.
35. Altman,S., Wesolowski,D., Guerrier-Takada,C. and Li,Y. (2005) RNase P cleaves transient structures in some riboswitches. *Proc. Natl Acad. Sci. USA*, **102**, 11284–11289.
36. Jensen,K.G. (1993) The *Escherichia coli* K-12 "wild types" W3110 and MG1655 have an *rph* frameshift mutation that leads to pyrimidine starvation due to low *pyrE* expression levels. *J. Bacteriol.*, **175**, 3401–3407.